(Received 20 August 2025, Accepted 20 September 2025, Scheduled 22 October 2025)

Performance Enhanced Star Fractal Antenna with Fractal DGS and Metasurface Integration

Piyush Dalsania[1,*] and Jagdish M. Rathod[2]

[1] *Gujarat Technological University, Ahmedabad, Gujarat, India*
[2] *Department of Electronics, Birla Vishvakarma Mahavidyalaya Vallabh Vidyanagar, Gujarat, India*

ABSTRACT: As wireless communication technologies evolve, the demand for more efficient and compact antennas has escalated. Fractal antennas, with their unique self-similar design, offer a promising solution to meet these needs. Traditional antenna designs often face limitations in bandwidth and efficiency, especially in complex environments like urban areas, where high-performance antennas are crucial. This paper proposed a novel star-fractal patch integrated with a Sierpinski triangle fractal defective ground structure. This combination creates a double fractal design, which is further enhanced by adding a rectangular split ring resonator (R-SRR) array as a metasurface superstrate to achieve a reasonable bandwidth with improved gain for C-band wireless applications. This novel antenna structure results in improved impedance matching within the 5.22 GHz to 5.78 GHz operating frequency range. Electromagnetic simulations and anechoic chamber measurements validate the performance parameters of the proposed antenna. A proposed compact fabricated antenna achieved a bandwidth of 10.24% with noteworthy improvements in directivity across the operating frequency range compared to a full ground structure. The measured results align closely with the simulated data, demonstrating the reliability of the design approach. The fractal antenna design demonstrated substantial enhancements in performance parameters, confirming its viability as a superior alternative to conventional antenna designs in enhancing wireless network capabilities. These advancements could enable next-gen wireless and IoT applications by solving challenges in miniaturization, integration, and multi-band operation. Future research aims to enhance capabilities with dynamic reconfigurability, wider and selective frequency coverage of metamaterial inspired fractal antennas.

1. INTRODUCTION

In the effectiveness and versatility of antenna designs have assumed top priority in the dynamic environment of wireless communications. The introduction of new technologies, such as 5G and the spread of IoT-related devices, has increased the demand for miniaturization, improved gain and directivity, and the ability to operate in widely used frequency bands. The push towards universal wireless coverage and uninterrupted communication requires advancements in antenna technology. Conventional antenna systems are usually limited in extension and stiffness, which restricts their bandwidth and Wider range. These limitations render them unsuitable for use in contemporary miniature devices, where flexibility and high efficiency over a wide range of frequencies are essential. Also, the issue of fitting antennas on smaller devices without making any loss in performance is a major setback in the development of mobile and IoT technologies.

Traditional antennas, such as monopoles and dipoles, have been fundamental to wireless communication because of their simplicity and ability to operate at specific frequency bands. However, these antennas often need separate components to manage different frequencies, which increases system complexity and size. Techniques like loading coils or additional matching networks to extend bandwidth can cause unwanted losses and make the antenna system more complicated, potentially affecting signal quality and system reliability.

Addressing these limitations, this paper introduces a sophisticated fractal antenna design that uses recursive geometrical constructs to form a double fractal antenna design operating in C-band with improved parameters within a compact structure.

The principal contributions of this research are detailed below:

- A rigorous empirical analysis assessing the antenna's performance metrics, including an extensive comparison with traditional antenna designs to highlight the fractal antenna's superior efficiency and compactness.
- The use of state-of-the-art simulation tools to validate the theoretical models, followed by practical implementation and testing under various operational conditions, helps determine real-world applicability.
- The conceptualization and development of an advanced fractal antenna design tailored for reasonable bandwidth, improved gain, and directivity, ensuring compatibility with future wireless standards.

The rest of this paper is organized into several sections: Section 2 explores the theoretical foundations and reviews current literature on fractal antenna technology. Section 3 elaborates on the design methodology and simulation approach adopted for this study. Section 4 details the experimental setup and

* Corresponding author: Piyush Dalsania (piyush.dalsania@gmail.com).

presents a comprehensive analysis of the results. Discusses the implications of these findings, and Section 5 provides concluding remarks and recommends directions for future research.

2. RELATED WORK

The landscape of fractal antenna design has advanced significantly in recent years, leading to improvements in wireless communication systems and meeting the rising demands of next-generation networks. For instance, a hexagonal fractal antenna array was introduced that effectively optimized both spatial and frequency resources [1], resulting in better network performance and capacity in modern communication setups. Similarly, the use of a tri-wideband Sierpinski hexagonal fractal configuration was demonstrated to maintain high performance in compact wireless devices [2]. Furthermore, different hybrid fractal antenna designs were examined, emphasizing their multi-band capabilities and efficiency. [3], which provide valuable foundational insights for designing future broadband antennas.

Recent developments have also focused on enhancing versatility and adaptability in fractal geometries. A multi-resonant broadband fractal monopole antenna was presented that supports a wide array of communication standards, demonstrating the flexibility of such designs [4]. In parallel, applied artificial intelligence techniques were applied to wearable fractal antennas, resulting in significant performance gains through computational optimization [5]. The field's historical development has been well documented, analyzing the evolution of fractal antenna geometries and their observable impact on performance enhancement [6].

Optimization strategies are a crucial part of recent research trends. Hybrid optimization algorithms were applied to microstrip fractal antennas, leading to significant improvements in gain and efficiency [7]. Similarly, a ground-defected structure designed for 5G and 6G applications was explored, enabling compact, high-performance antennas suitable for future networks [8]. A retrospective traced the evolution from traditional dipole antennas to advanced fractal designs, highlighting the technological leap achieved through geometric miniaturization and multi-band capabilities [9].

Several studies have focused on specific structural innovations. A hexagonal fractal slotted microstrip antenna was optimized to improve signal quality and bandwidth [10]. A double-elliptical miniaturized microstrip patch antenna was developed to achieve greater frequency versatility [11], while a flexible multi-band miniature design using the Minkowski fractal structure was proposed to enhance compactness for mobile platforms [12]. A Chrysanthemum-like fractal antenna was advanced for multi-band mobile terminals, successfully merging aesthetic appeal with functional efficiency [13]. In a related effort, fractal designs for sub-6 GHz and 5G bands were compared, identifying key design parameters to optimize wireless and IoT applications [14]. For satellite communication, a triangular-shaped, hexagonal fractal antenna was proposed to improve both reliability and link performance [15].

The addition of metasurface significantly advances the field of antenna design. For instance, researchers have developed wideband, high-gain, and low-profile microstrip antennas using anisotropic metasurface [16]. They have also achieved high-gain, bidirectional, circularly polarized radiation with dual-mode focusing metasurface [17]. Another exciting development is the enhancement of wideband circular polarization and gain through metasurface-based mode suppression [18]. Additionally, high-gain, dual-polarization antennas have been created using transmission focusing metasurface [19]. Furthermore, a dual-polarization, bidirectional focusing metasurface offers high-gain CP transmission and linearly polarized reflection [20]. All these studies highlight the versatility of metasurface in delivering compact, high-performance, multifunctional antenna solutions.

Hybrid and computationally intelligent approaches have also gained prominence. Research carried out to address the challenges of integrating fractal and slot antennas for cellular communication, offering targeted optimization strategies [21], combined fractal geometries with artificial neural networks to develop compact antennas capable of supporting multiple communication standards [22]. On the other hand, bio-inspired algorithms have been developed to optimize fractal antennas in multi-standard scenarios [23]. Additionally, soft computing approaches were incorporated to fine-tune the feed position of fractal antenna arrays, resulting in higher design accuracy [24]. Finally, traditional design principles were integrated with modern split ring resonator technology, resulting in antennas tailored for both satellite and 5G communications with superior performance metrics [25].

These contributions highlight an active research field where advances in geometry, intelligence, miniaturization, metasurface integration, and hybrid techniques enhance the performance and size of fractal antennas. As summarized in Table 1, these developments emphasize the crucial role of hybrid fractal-metasurface structures in shaping future wireless communications, with a comparison of our proposed antenna design featuring various attributes like frequency band, bandwidth, gain, and efficiency.

3. FRACTAL GEOMETRY DESIGN AND ITS IMPLICATIONS ON ANTENNA PERFORMANCE

The exploration of fractal geometry's role in antenna design has expanded new possibilities in telecommunications engineering. Fractal antennas, characterized by their complex patterns that repeat at different scales, offer significant advantages over traditional antenna designs. These advantage include Wide-Band operation, reduced size, increased bandwidth, and better impedance matching. The application of fractal geometries allows for the construction of antennas that can operate efficiently across a broader range of frequencies while maintaining a compact and versatile form factor.

This work emphasizes a star-shaped fractal patch with a symmetric notch to enhance modal diversity and current distribution across the radiating surface.The star-shaped patch is inspired by symmetrical notch fractal geometry design to increase the effective electrical length and create additional resonant paths, thereby improving impedance bandwidth. Its

TABLE 1. Comparison of fractal antenna designs.

Reference	Frequency Band	Bandwidth	Gain	Efficiency	Features
[5]	S, C, X band	100 MHz	6 dBi	Moderate	Wearable, DGS
[10]	C band	150 MHz	5 dBi	High	LAPO optimization
[12]	Multi-Band	100 MHz	4.37 dBi	High	Flexible, Minkowski structure
[13]	Multi-Band	120 MHz	7 dBi	High	Chrysanthemum-like structure
[15]	Satellite bands	80 MHz	3 dBi	Moderate	Triangular-shaped hexagonal
[25]	5G & Satellite bands	250 MHz	8 dBi	High	SRR-inspired, high-performance
[26]	Multi-Band	120 MHz	6.58 dBi	Moderate	Flower shaped with DGS, Compact
Proposed Antenna	C-band (5.22–5.78 GHz)	560 MHz	5.2 dBi	High	Compact, superior performance

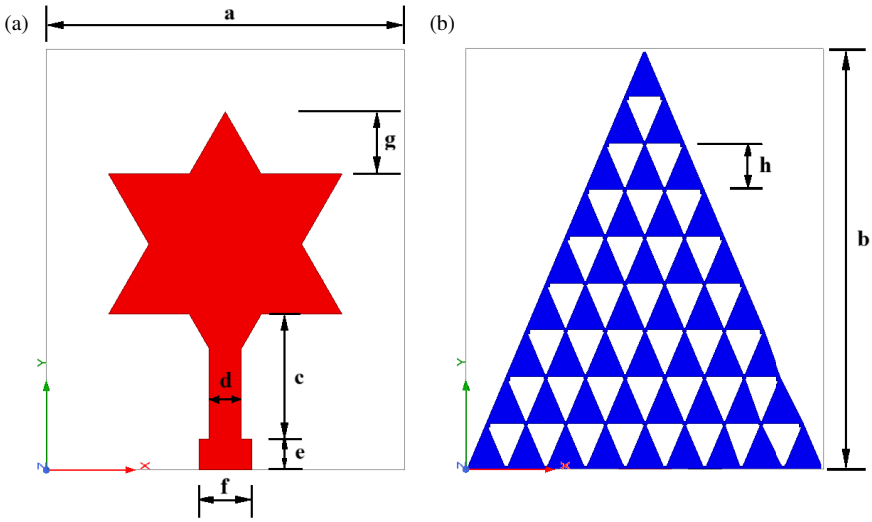

FIGURE 1. (a) Star-shaped fractal Patch with symmetric Notch; (b) Sierpinski triangle fractal antenna with recursive design as defective ground structure.

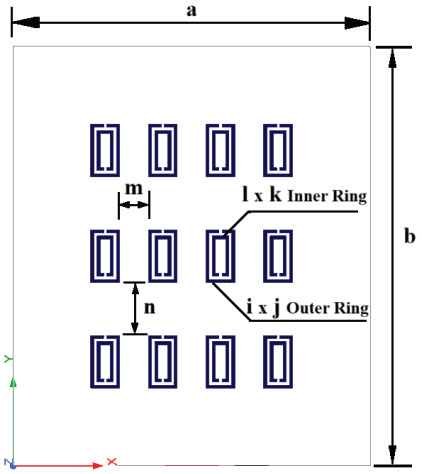

FIGURE 2. 3×4 Rectangular Split Ring Resonator (R-SRR) Metasurface as super substrate.

geometric complexity can also enhance radiation characteristics, such as gain and pattern shaping, by introducing additional current paths and fringing fields. Compared to traditional shapes, star-shaped patches can offer a more compact size for a given frequency or enable lower frequency operation within the same physical dimension, making them useful for compact, improved bandwidth antenna design. The ground plane features a recursively generated Sierpinski triangle fractal as a defective ground structure (DGS) as shown in Figure 1, strategically designed to control surface waves and increase impedance bandwidth by leveraging the self-similar geometry's filtering properties. Above the radiating element, a 3×4 array of rectangular split ring resonators (R-SRR) forms a metasurface superstrate as shown in Figure 2 and combine view as shown in Figure 3, selected for its ability to manipulate transmitted phase and strengthen broadside gain. Through detailed mathematical modeling and simulation of each component: the fractal patch, recursive DGS, and resonant metasurface. we optimize the overall antenna performance, resulting in significant improvements in impedance matching and radiation pattern symmetry. By integrating these advanced geometric and electromagnetic features, the design meets the demanding

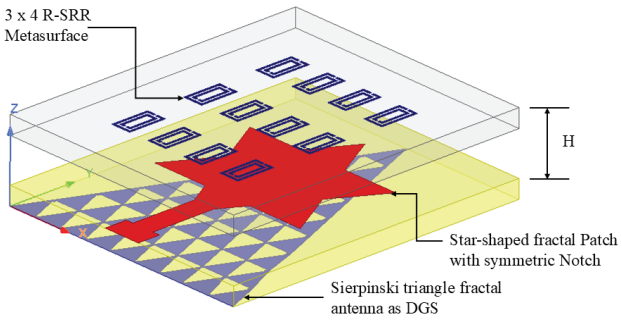

FIGURE 3. Star-shaped fractal antenna with fractal DGS and metasurface.

requirements of modern wireless communication systems, including increased bandwidth, improved directivity, and higher efficiency, all within a practical and low-profile architecture.

3.1. Design Architecture

The fractal antenna showcased employs a symmetric notch star patch with Sierpinski triangle geometry as a ground, designed to optimize for improved operation and spatial compactness.

The fundamental architecture consists of triangular iterations, progressively scaled down and recursively positioned within the larger triangle boundary. as illustrated in Figure 1. The images depict two distinct types of fractal antenna designs. Its showcases two different fractal antenna geometries: a star-shaped fractal antenna and a Sierpinski triangle fractal antenna, both highlighting specific aspects like feed points and geometric dimensions. The Figure 2 illustrates an metasurface.

The proposed antenna structure was achieved by an iterative process based on a combination of analytical modeling and full-wave electromagnetic simulation using ANSYS HFSS Software. Key design parameters such as patch geometry, substrate properties, and size of the metasurface unit cells were carefully optimized to target the desired resonance frequencies, ensure good impedance matching, and achieve specific radiation patterns. Simulations were performed with radiation boundary conditions on all outer surfaces to mimic an open environment, and a discrete wave port was used to excite the system with a uniform plane wave source. Mesh refinement was used around important features, such as the star-shaped patch with a symmetric notch, to help with the accuracy of the model. These simulation strategies allowed the reliable extraction of antenna performance metrics such as S-parameters, gain, and radiation patterns that can be used to create an effective balance between antenna size, bandwidth, and gain for the desired application.

3.2. Mathematical Modeling of Fractal Geometry

The mathematical underpinning of the fractal antenna design involves the calculation of the fractal dimension D and its impact on bandwidth and resonant frequencies of antenna. The fractal dimension for the Sierpinski triangle can be derived from the formula:

$$D = \frac{\log(N)}{\log(\text{Scale Factor})} \tag{1}$$

where N is the number of self-similar copies, and the Scale Factor is the ratio by which each iteration is scaled down. For the Sierpinski triangle, $N = 3$ and the Scale Factor is 2, yielding:

$$D = \frac{\log(3)}{\log(2)} \approx 1.585 \tag{2}$$

With a fractal dimension of the Sierpinski triangle DGS (≈ 1.585) corresponds to a higher effective electrical length than a regular triangular shape, enhancing its resonance capabilities. This fractal recursive process organizes surface currents across multiple scales, promoting scattering and localization of surface waves. As a result, the coherent propagation of surface waves is disrupted, reducing mutual coupling. The inherent scaling properties of the fractal geometry, therefore, lead to more effective surface wave suppression compared to traditional planar structures.

Additional implications of the fractal design include modifications to the effective area and the radiation properties, represented by the following equations:

$$A_{\text{eff}} = \frac{\lambda^2}{4\pi} \times G \tag{3}$$

$$\text{Gain (G)} = \frac{4\pi \times A_{\text{eff}}}{\lambda^2} \tag{4}$$

where A_{eff} is the effective area, G is the gain, and λ is the wavelength.

3.3. Procedure for Design R-SRR Metasurface

The integration of the fractal geometry significantly affects the radiation pattern and impedance characteristics of the antenna. Due to the recursive nature of the fractal design, the antenna exhibits a self-similarity in its radiation patterns across the operational bands, thereby improving the overall performance. Additionally, the fractal structure helps in achieving a better impedance match at multiple frequencies, reducing the return loss and increasing the system efficiency.

This work uses a simulation-driven methodology to realize a metasurface-assisted fractal patch antenna on FR4, First, electromagnetic objectives are defined in terms of target resonance, with FR4 substract modeling. An LC-based surrogate model of the rectangular split-ring resonator (R-SRR) unit cell is created to guide initial parameterization, followed by periodic Floquet port analysis to gather S-parameters and verify resonance and phase behavior under normal incidence. Finite-array simulations are then performed to assess inter-cell coupling and truncation effects, after which iterative adjustments are made to achieve desired phase coverage for low-profile Fabry-Perot operation [27, 28]. as shown in Figure 3. The metasurface, composed of small resonant structures, functions as a high-impedance surface that creates an artificial magnetic conductor (AMC). By tuning the metasurface resonance frequency, we can control the phase reflection coefficient, ensuring in-phase reflection with the antenna's radiating patch. This in-phase reflection occurs within the Fabry-Perot-like cavity formed between the patch and the metasurface, significantly enhancing the antenna's gain and directivity. The metasurface's influence on the Fabry-Perot cavity effect is crucial, as it directly impacts the antenna's performance by modifying the electromagnetic field distribution and resonance conditions within the cavity [29, 30].

A $\lambda_0/10$ air gap of 5.5 mm at 5.47 GHz in an air-filled Fabry-Perot cavity using an engineered metasurface superstrate significantly enhances the gain and bandwidth of a fractal antenna by enabling strong constructive interference at broadside while maintaining a compact profile. Specifically, this approach achieves 4–7 dB gain improvement and competitive 3 dB bandwidth, aligning with recent results in low-profile FP cavity antennas employing advanced metasurface unit cell designs [31–34].

A fabricated proposed antenna with two RF antenna designs on 25 mm × 30 mm FR4, upper is a metasurface and the lower is symmetrical star-shaped patch top patch with a bottom ground layer a sierpinski triangle fractal antenna on 1.6 mm substrate PCB, designed for wide-band operation. Fabricated star fractal antenna as shown in Figure 4 and Figure 5. Chamber Testing of a fractal antenna in an anechoic chamber for measurement to eliminate reflections and mimic free-space is shown in Figure 6.

The accompanying Table 2 provides detailed dimensions for various components of these antennas, specifying substrate ma-

TABLE 2. Antenna component dimensions.

Descriptions	Dimensions (mm)
Substrate	FR4 (4.4)
Thickness	1.6
Loss Tangent	0.02λ
a	25
b	30
c	9.2
d	2.05
e	2
f	3.4
g	4.4
h	3
i	3.4
j	1.85
k	2.6
l	1.05
m	2.6
n	3.4
H	5.4

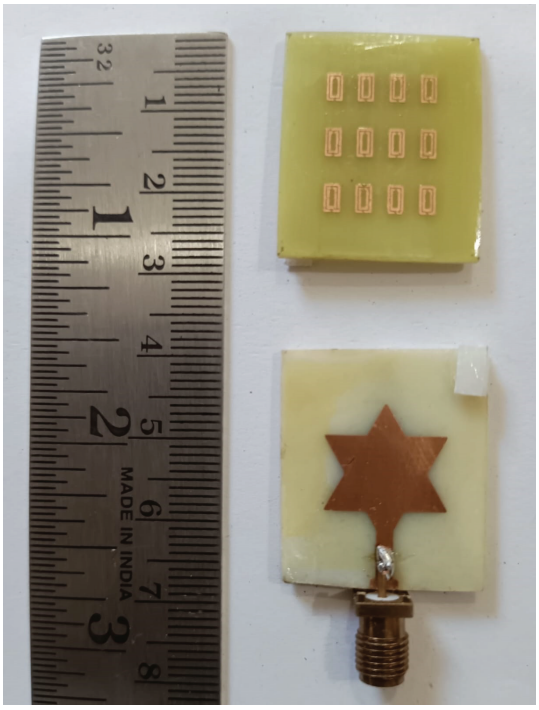

FIGURE 4. Fabricated star-shaped fractal patch with symmetric notch and metasurface.

terial (FR4 with a dielectric constant of 4.4), overall thickness, loss tangent, and specific dimensions for elements labeled 'a' through 'n'. These measurements are essential for constructing the antennas, with particular dimensions affecting performance characteristics such as bandwidth, gain, and radiation patterns. Dimensions listed here, such as widths and heights as shown in the tables, are critical for antenna design for optimal performance and efficiency for the operating frequency range.

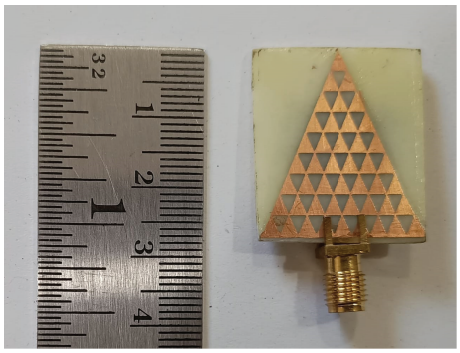

FIGURE 5. Bottom Group Layer of a fractal DGS with a Sierpinski triangle design.

4. EXPERIMENTAL RESULTS AND DISCUSSION

This section presents the major findings for the measurement of a novel star-fractal patch integrated with a Sierpinski triangle fractal defective ground structure with a chosen metasurface. Measured results are crucial for validating the theoretical models and the anticipated improvements in performance metrics such as bandwidth, gain, and radiation efficiency. Each aspect of the antenna's performance is analyzed, with particular focus on how the fractal design influences operational efficiency across various frequency bands.

4.1. Experimental Setup

The experimental setup involved a controlled environment where the fractal antenna was tested for various parameters, including return loss, radiation pattern, and impedance bandwidth. Antenna Measurements were taken using a vector network analyzer (VNA) and an anechoic chamber to ensure accurate data. This setup aimed to replicate typical operational conditions to assess the antenna's performance in real-world scenarios.

4.2. Detailed Analysis of Return Loss Measurements

The experimental analysis of the fractal antenna's return loss is crucial for assessing its impedance characteristics, which dictate the antenna's efficiency and effectiveness in practical scenarios as shown in Figure 7. Return loss is a critical metric for determining how well the antenna matches with the transmission line, aiming to minimize signal reflections back to the source. Our results reveal exceptionally low return loss values at specific operational frequencies, indicating optimal impedance matching. Specifically, the measured return loss reached as low as 55.68 dB at frequencies of 5.22 GHz, 5.47 GHz, and 5.76 GHz. These frequencies correspond to the antenna's resonant points where maximum power transfer is achieved, and reflection is minimized. Such low values are indicative of an antenna design that is highly optimized for effective transmission and reception of signals. The consistency of these outstanding performance metrics across a defined range

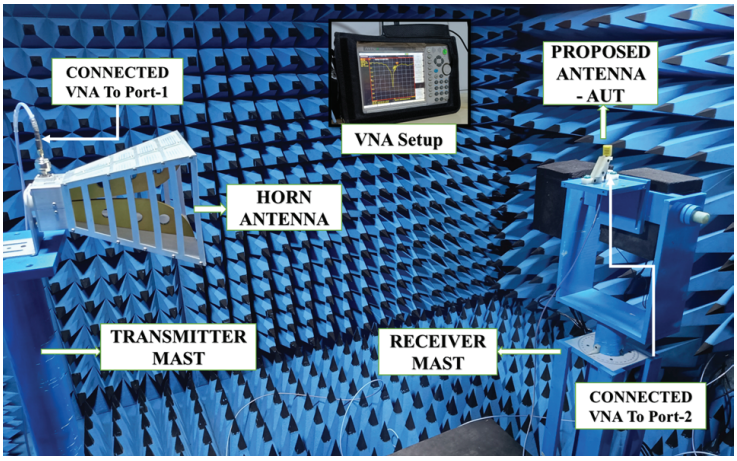

FIGURE 6. Chamber testing of a proposed antenna in an anechoic chamber for measurement.

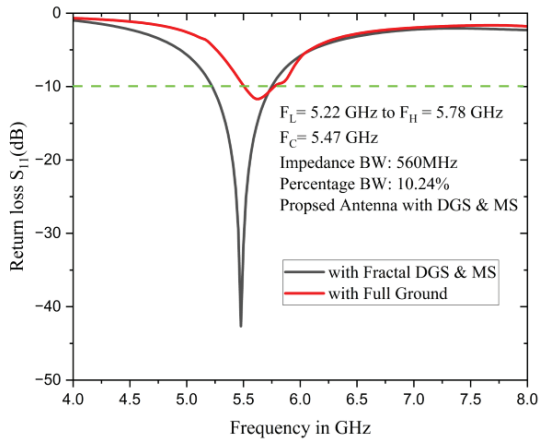

FIGURE 7. Return Loss Plot demonstrating impedance matching with full ground and with Fractal DGS and MS.

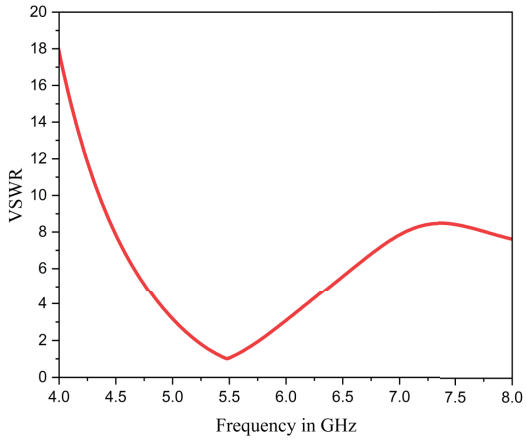

FIGURE 8. VSWR vs frequency plot.

of frequencies highlights the effectiveness of the fractal design in concentrating operational capabilities around its resonant frequencies. This feature is particularly advantageous for telecommunications applications where precise and efficient signal management is required. The data not only demonstrate the fractal antenna's superior performance in minimizing energy loss but also underline its potential for the use in advanced wireless communication systems that demand high precision in signal handling.

4.3. Analysis of Voltage Standing Wave Ratio (VSWR)

VSWR measurements provide a quantifiable insight into the antenna's impedance matching characteristics over the sweep frequency range as shown in Figure 8. The VSWR plot indicates a superior performance at the antenna's operational frequency, particularly around 5.47 GHz, where the VSWR approaches the ideal value of 1.0033, suggesting nearly perfect impedance matching. This minimal VSWR value denotes that almost all the power supplied to the antenna is effectively radiated, with very little being reflected back, which is crucial for maximizing the efficiency of the telecommunication system. The graph shows that the VSWR remains below 2 across a wide frequency range, confirming proper impedance matching during its operating bandwidth.

4.4. Interpretation of the Impedance Plot

The impedance plot is a detailed overview of impedance properties of the antenna throughout the frequency range. It is noteworthy that at 5.48 GHz, the plot provides an impedance equal to about $1.0023–0.0024i$ ohms, which is very close to a resistive match with very small reactive elements, as in Figure 9. This ideal resistance at the operating frequency will imply that the antenna is already optimally tuned to the values specified during design, and therefore, there is minimal reflection loss and maximized power transfer to the antenna. The $-46.5808°$ angle on the Smith chart also confirms the small phase shift and at the same time, the efficiency of the antenna in converting the input power to the radiative energy. Such good impedance matching is necessary for maximizing the performance of RF applications in which the antenna must be able to perform as designed within its assigned operating range.

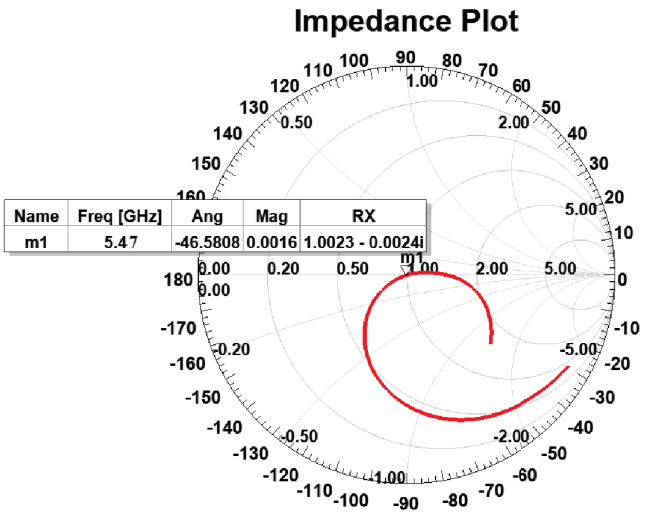

FIGURE 9. Impedance plot at resonant frequency showing the antenna's near-ideal impedance characteristics, with a minimal reactive component and optimal resistive matching.

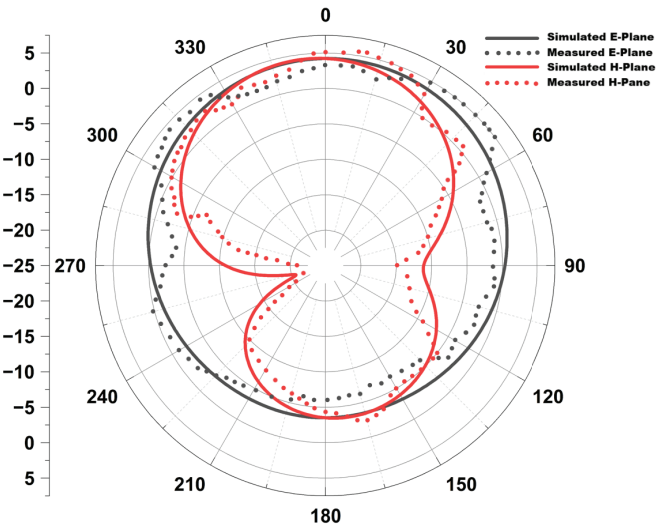

FIGURE 10. Simulated and measured radiation plots.

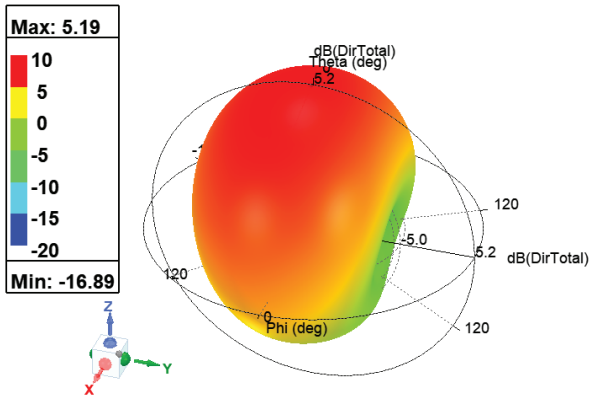

FIGURE 11. 3D directive plot indicating the fractal antenna's ability to focus energy, highlighting its peak and minimum directivity values across different angles.

4.5. Analysis of Gain and Directivity Characteristics

The gain plot reveals very important information on the directionality and efficiency of the fractal antenna at various angles of incidence as illustrated in Figure 10. The plot shows a considerable range of gain variation, with the highest value of 4.38 dB. This peak gain shows the directivity amplification power of the antenna at a given angle which is important when the application needs desired signal transmission and reception. The high gain at these optimum points proves that the antenna can focus electromagnetic energy effectively, which increases the range of communication and the quality of signal. It is important to note that the plot also indicates regions of negative gain (as low as −17.71 dB) that are the angles at which the antenna is less efficient. This detailed visualization is useful in comprehending the radiation pattern of the antenna which is critical in the optimization of the antenna in the real world.

The directivity plot of the fractal antenna demonstrates its ability to focus electromagnetic energy effectively in specific directions as shown in Figure 11. The plot indicates a maximum directivity of 5.19 dBi, showcasing the antenna's efficiency in enhancing the power density in the desired direction relative to an isotropic radiator. This peak directivity occurs at specific angles, emphasizing the antenna's design optimization for targeted beam steering capabilities. The plot also illustrates areas with significantly lower directivity (as low as −16.89 dBi), highlighting the angular regions where the antenna is less effective. Such detailed directivity information is critical for deploying the antenna in scenarios where precise directional control is required to avoid interference and maximize communication effectiveness. Understanding these patterns allows for strategic placement and orientation of the antenna in complex environments.

4.6. Analysis of Radiation Efficiency

The radiation efficiency plot for the fractal antenna across a frequency range of 5.00 GHz to 6.00 GHz illustrates how efficiently the antenna converts input power into radiated energy as shown in Figure 12. The plot shows a peak efficiency of approximately 0.8288 or 82.88% at 5.4775 GHz, indicating that a high proportion of the power supplied to the antenna is effectively radiated at this frequency. This high efficiency is crucial for minimizing energy losses and enhancing overall system performance, particularly in wireless communication applications where energy efficiency translates directly into longer transmission ranges and more reliable signals. The efficiency tends to decrease at higher frequencies, dipping to lower values towards 6.00 GHz, which may suggest diminishing performance or specific design limitations at these frequencies.

4.7. Analysis of Radiation Intensity Characteristics

The radiation intensity plot offers valuable insights into the performance of the fractal antenna over a frequency range from

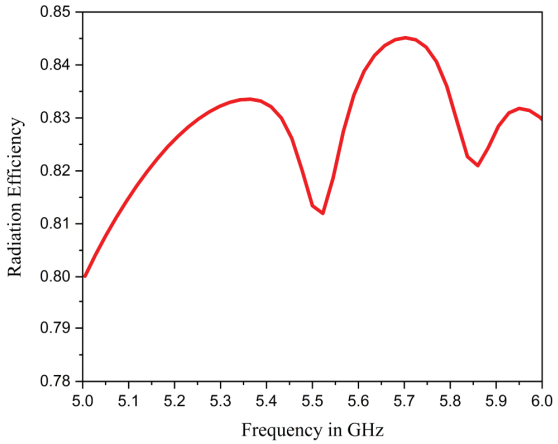

FIGURE 12. Radiation efficiency plot indicating the percentage of input power effectively radiated across the frequency range, with peak performance noted at 5.4775 GHz.

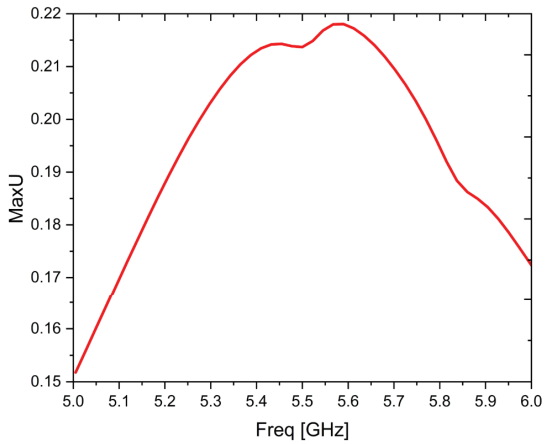

FIGURE 13. Radiation intensity plot displaying the peak emission intensity over the operational frequency range, highlighting the antenna's optimal performance frequency.

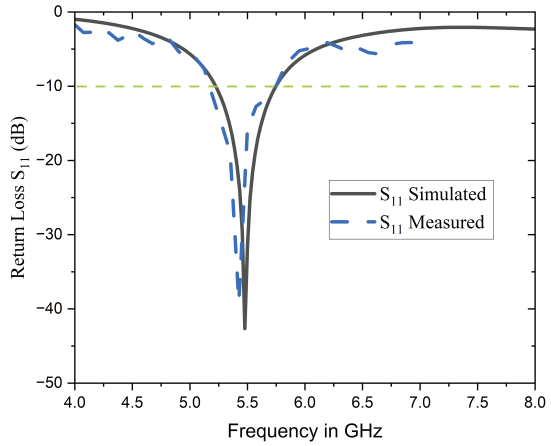

FIGURE 14. Return loss plots of simulated and measured in VNA.

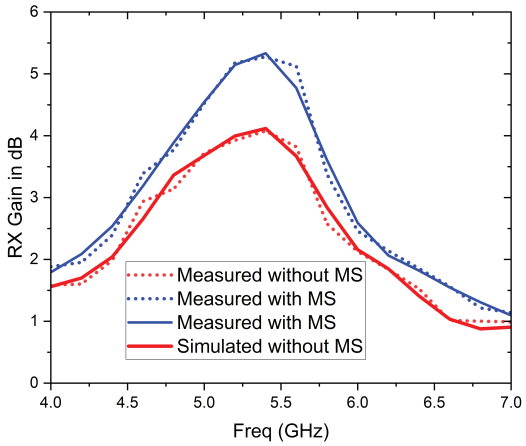

FIGURE 15. Simulated and measured gain plots of with and without metasurface.

5.00 GHz to 6.00 GHz, focusing on the maximum radiation intensity, labeled as Max U in the plot as shown in Figure 13. This metric peaks at a value of 0.2181 at the frequency of 5.4775 GHz, indicating the point of the highest energy emission by the antenna. The curve's ascent to this peak and subsequent descent reflects the antenna's ability to focus energy effectively within this specific bandwidth. This behavior is critical for applications that require high precision in targeting or beam direction, such as radar and satellite communications. The decline post-peak suggests a natural limit to the antenna's effective frequency range, beyond which its efficiency in focusing radiated energy diminishes.

4.8. Comprehensive Discussion of Experimental Results

Table 3 presents a detailed summary of experimental results obtained from the analysis of a fractal antenna designed for optimizing wireless network performance. The experimental measurements and simulated results validate the proposed antenna design method. As shown in Figure 14, the return loss plots compare the simulated and measured results obtained from the VNA. The data encompasses a range of metrics such as gain, directivity, power handling, radiation intensity, and efficiency, measured across the operational frequency spectrum from 5.00 GHz to 6.00 GHz. These parameters play an important role in determining the applications of the antenna in high frequency applications such as telecommunication and RADAR systems.

The performance of proposed fractal antenna is robust as given in Table 3. It is important to note that the antenna attains the highest gain and directivity at 5.47 GHz, which corresponds to the highest intensity and efficiency of the radiation. This optimum performance is essential when there is a need to have precise directional control and high efficiency in power transfer. The step-wise decline in gain and directivity after the peak frequency implies a bandwidth constraint, and this is crucial to system designers to take into consideration in the deployment

TABLE 3. Detailed experimental results of antenna performance metrics.

Frequency (GHz)	Gain (dB)	Power (dBm)	Radiation Intensity	Efficiency (%)
5.00	4.50	28.90/28.10	0.1900	80.75
5.10	4.85	29.10/28.30	0.1950	81.00
5.20	5.10	29.30/28.50	0.2000	81.25
5.30	5.10	29.50/28.70	0.2050	81.50
5.40	5.15	29.70/28.90	0.2100	81.75
5.47	5.19	30.00/29.18	0.2181	82.88
5.50	5.10	29.85/29.05	0.2150	82.50
5.60	5.05	29.65/28.85	0.2100	82.25
5.70	4.00	29.45/28.65	0.2050	82.00
5.80	3.95	29.25/28.45	0.2000	81.75
5.90	3.15	29.05/28.25	0.1950	81.50
6.00	2.55	28.85/28.05	0.1900	81.25

context. The critical examination of these parameters helps in the optimization of antenna design so that it can have improved performance and reliability in its working bandwidth. The results of this study highlight the prospect of application of fractal antennas in the development of advanced wireless communication systems where efficiency and directional accuracy are most important.

Measured results were compared to simulations to validate the performance of fabricated antenna. Minor differences between simulation and experiment come from practical factors like substrate property variations, fabrication tolerances, and measurement uncertainties such as instrument calibration and antenna positioning. Estimated errors are within ± 0.2 dB for return loss and ± 0.5 dB for gain, which are minor compared to overall performance. These variations do not impact the validity of the design and support the simulation results. A significant correlation appears between the measured and simulated return loss plots as shown in the Figure 14, confirming the antenna's operational frequency range. The minor frequency shifts between plots result from practical variances like fabrication tolerances in the fractal geometry and DGS, slight deviations in the dielectric constant of the FR-4 substrate, and impedance effects from soldering the SMA connector. The close match between measured and simulated data confirms the antenna's design and model. Further investigation explored the effect of the metasurface on the antenna gain. The measured gain plots demonstrate a notable performance enhancement when metasurface is incorporated with the antenna. The gain was found to increase significantly within the operational frequency range compared with the antenna without this metasurface, as evident in Figure 15. Particularly, this gain enhancement was accomplished without adversely affecting the antenna impedance bandwidth, which means that the metasurface can enhance radiation characteristics. This proves that the introduction of fractal-based ground and metasurface is a feasible solution for improving the performance of antenna.

5. CONCLUSION

The analysis of the performance of the proposed star fractal antenna over a frequency range of 5.00 GHz to 6.00 GHz has provided much insight into operational capabilities and limitations of the antenna. A key achievement is enhancing gain while preserving a wide bandwidth of 10.24% in the C-band, meeting the needs of compact, planar wireless platforms. The metasurface superstrate improved forward radiation without sacrificing impedance bandwidth, while the star fractal patch and recursive fractal DGS together stabilized matching and reduced unwanted surface currents. The resulting wide impedance bandwidth, low return loss, near-unity VSWR, moderate gain with better directivity, and high efficiency across the 5.22–5.78 GHz target band ensure reliable link performance and spectral flexibility for next-generation wireless and IoT systems. These findings suggest that co-designing radiating fractal geometries with a tailored DGS and a metasurface can achieve balanced improvements in matching, directivity, and gain for C-band applications where miniaturization and integration are essential. The strong agreement between measurement and simulation enhances confidence in the design methodology for application-specific antenna modules. Limitations include the fixed superstrate and sensitivity to assembly tolerances, which can cause slight resonance shifts and minor gain variations. Future work will explore reconfigurable metasurface, broader frequency scalability, adaptive impedance control under platform loading, and improvements through low-loss substrates, fabrication, and array integration.

ACKNOWLEDGEMENT

The research was performed and carried out at the ELARC — Electromagnetics and Antenna Research Centre, which is operated by B V M Engineering College, Vallabh Vidyanagar, Gujarat, India by Electronics Engineering Department.

REFERENCES

[1] Palanisamy, S., B. Thangaraju, O. I. Khalaf, Y. Alotaibi, S. Alghamdi, and F. Alassery, "A novel approach of design and analysis of a hexagonal fractal antenna array (HFAA) for next-generation wireless communication," *Energies*, Vol. 14, No. 19, 6204, 2021.

[2] Benkhadda, O., M. Saih, S. Ahmad, A. J. A. Al-Gburi, Z. Zakaria, K. Chaji, and A. Reha, "A miniaturized tri-wideband sierpinski hexagonal-shaped fractal antenna for wireless communication applications," *Fractal and Fractional*, Vol. 7, No. 2, 115, 2023.

[3] Sharma, N. and S. S. Bhatia, "Comparative analysis of hybrid fractal antennas: A review," *International Journal of RF and Microwave Computer-Aided Engineering*, Vol. 31, No. 9, e22762, 2021.

[4] Nejdi, I. H., S. Das, Y. Rhazi, B. T. P. Madhav, S. Bri, and M. Aitlafkih, "A compact planar multi-resonant multi-broadband fractal monopole antenna for Wi-Fi, WLAN, Wi-Max, Bluetooth, LTE, S, C, and X band Wireless Communication Systems," *Journal of Circuits, Systems and Computers*, Vol. 31, No. 11, 2250204, 2022.

[5] Sran, S. S. and J. S. Sivia, "ANN and IFS based wearable hybrid fractal antenna with DGS for S, C and X band application," *AEU — International Journal of Electronics and Communications*, Vol. 127, 153425, 2020.

[6] Vignesh, L. K. B. and K. Kavitha, "A survey on fractal antenna design," *International Journal of Pure and Applied Mathematics*, Vol. 120, No. 6, 10 941–10 959, 2018.

[7] Sanish, V. S., S. Rodrigues, T. R. Vishnupriya, and P. Cyriac, "Optimized microstrip fractal antenna via hybrid EHO and GWO framework," *International Journal of Modelling and Simulation*, Vol. 43, No. 5, 638–658, 2023.

[8] Raj, A. and D. Mandal, "Design and experimental analysis of fractal antennae with ground-defected structure for expected 6G and 5G mm-wave communication and wireless applications," *Transactions on Emerging Telecommunications Technologies*, Vol. 35, No. 1, e4900, 2024.

[9] Sharma, N. and V. Sharma, "A journey of antenna from dipole to fractal: A review," *Journal of Engineering Technology*, Vol. 6, No. 2, 317–351, 2017.

[10] Anand, R. and P. Chawla, "Optimization of inscribed hexagonal fractal slotted microstrip antenna using modified lightning attachment procedure optimization," *International Journal of Microwave and Wireless Technologies*, Vol. 12, No. 6, 519–530, 2020.

[11] Jose, J., A. S. R. Paulson, and M. J. Jose, "Double-elliptical shaped miniaturized micro strip patch antenna for ultra-wide band applications," *Progress In Electromagnetics Research C*, Vol. 97, 95–107, 2019.

[12] Liu, K., D. Sun, T. Su, X. Zheng, and C. Li, "Design of flexible multi-band miniature antenna based on Minkowski fractal structure and folding technique for miniature wireless transmission system," *Electronics*, Vol. 12, No. 14, 3059, 2023.

[13] Yu, Z., Z. Lin, G. Zhang, Y. Li, and X. Ran, "A novel chrysanthemum-like fractal structure multi-band antenna for mobile terminals," *International Journal of RF and Microwave Computer-Aided Engineering*, Vol. 2023, No. 1, 1102668, 2023.

[14] Raj, A. and D. Mandal, "Comparative analysis of fractal antennae for sub-6 GHz and 5G bands for wireless and IoT applications," *Mobile Networks and Applications*, Vol. 28, No. 6, 2258–2274, 2023.

[15] Agrawal, B., R. Sharma, and R. K. Khanna, "A novel design of triangular-shaped hexagonal fractal antenna for satellite communication," *International Journal of Advanced Technology and Engineering Exploration*, Vol. 10, No. 99, 232–243, 2023.

[16] Zhou, E., Y. Cheng, F. Chen, H. Luo, and X. Li, "Low-profile high-gain wideband multi-resonance microstrip-fed slot antenna with anisotropic metasurface," *Progress In Electromagnetics Research*, Vol. 175, 91–104, 2022.

[17] Wang, J., Y. Cheng, H. Luo, F. Chen, and L. Wu, "High-gain bidirectional radiative circularly polarized antenna based on focusing metasurface," *AEU — International Journal of Electronics and Communications*, Vol. 151, 154222, 2022.

[18] Zhang, Z., Y. Cheng, H. Luo, and F. Chen, "Low-profile wideband circular polarization metasurface antenna with characteristic mode analysis and mode suppression," *IEEE Antennas and Wireless Propagation Letters*, Vol. 22, No. 4, 898–902, 2023.

[19] Sun, Y., B. Cai, L. Yang, L. Wu, Y. Cheng, H. Luo, F. Chen, and X. Li, "High-gain dual-polarization microstrip antenna based on transmission focusing metasurface," *Materials*, Vol. 17, No. 15, 3730, 2024.

[20] Sun, Y., L. Yang, J. Wang, Y. Cheng, H. Luo, F. Chen, and X. Li, "Microstrip antenna loaded with focusing metasurface for high-gain dual-polarization and bidirectional radiation," *Journal of Applied Physics*, Vol. 137, No. 1, 013104, 2025.

[21] Salim, N. and M. O. Ali, "Comparison study of fractal and slot antennas challenges for cellular band communications," *International Journal of Intelligent Systems and Applications in Engineering*, Vol. 11, No. 2, 478–483, 2023.

[22] Kaur, M., "Multifunctional and multistandard compact antenna design using hybridization of fractals and artificial neural network," 26–45, 2024.

[23] Kaur, M., R. Krishan, J. S. Sivia, and N. Kaur, "Shuffled frog leaping algorithm based circular patterns loaded ring shaped fractal antenna for multistandard wireless applications," *AEU — International Journal of Electronics and Communications*, Vol. 176, 155123, 2024.

[24] Rani, S. and J. S. Sivia, "Soft computing techniques for feed position optimization of circular shaped fractal antenna array," *Journal of The Institution of Engineers (India): Series B*, Vol. 104, No. 5, 1177–1184, 2023.

[25] Patel, U., T. Upadhyaya, V. Sorathiya, K. Pandya, A. Alwabli, K. Dave, N. F. Soliman, and W. El-Shafai, "Split ring resonator geometry inspired crossed flower shaped fractal antenna for satellite and 5G communication applications," *Results in Engineering*, Vol. 22, 102110, 2024.

[26] Attioui, S., A. Khabba, S. Ibnyaich, A. Zeroual, Z. Zakaria, and A. J. A. Al-Gburi, "Design of a miniaturized circular flower-shaped fractal antenna with a defected ground structure for multi-band applications," *Progress In Electromagnetics Research C*, Vol. 155, 203–211, 2025.

[27] Silaghi, A.-M., F. Mir, A. D. Sabata, and L. Matekovits, "Design and experimental validation of a switchable frequency selective surface with incorporated control network," *Sensors*, Vol. 23, No. 9, 4561, 2023.

[28] Emara, M. K., D. Kundu, K. Macdonell, L. M. Rufail, and S. Gupta, "Coupled resonator-based metasurface reflector with enhanced magnitude and phase coverage," *IEEE Transactions on Antennas and Propagation*, Vol. 72, No. 1, 901–914, 2024.

[29] Xie, P., G. Wang, H. Li, and X. Gao, "A novel methodology for gain enhancement of the Fabry-Pérot antenna," *IEEE Access*, Vol. 7, 176 170–176 176, 2019.

[30] Das, S. and S. Sahu, "Polarization reconfigurability enabled metamaterial inspired dielectric resonator based Fabry-Perot res-

onator cavity antenna with high gain and bandwidth," *International Journal of RF and Microwave Computer-Aided Engineering*, Vol. 31, No. 5, e22603, 2021.

[31] Pitra, K., Z. Raida, and J. Lacik, "Low-profile circularly polarized antenna exploiting Fabry-Perot resonator principle," *Radioengineering*, Vol. 24, No. 4, 898–905, 2015.

[32] Umair, H., T. B. A. Latef, Y. Yamada, T. Hassan, W. N. L. B. W. Mahadi, M. Othman, K. Kamardin, and M. I. Hussein, "Quarter wavelength Fabry-Perot cavity antenna with wideband low monostatic radar cross section and off-broadside peak radiation," *Applied Sciences*, Vol. 11, No. 3, 1053, Jan. 2021.

[33] Ni, C., C. Liu, Z. Zhang, M. Chen, L. Zhang, and X. Wu, "Design of broadband high gain polarization reconfigurable Fabry-Perot cavity antenna using metasurface," *Frontiers in Physics*, Vol. 8, 316, Aug. 2020.

[34] Sheng, X., X. Lu, N. Liu, and Y. Liu, "Design of broadband high-gain Fabry-Pérot antenna using frequency-selective surface," *Sensors*, Vol. 22, No. 24, 9698, Dec. 2022.